BIOCHEMISTRY

Directed evolution of an α1,3-fucosyltransferase using a single-cell ultrahigh-throughput screening method

Yumeng Tan[1]*, Yong Zhang[1]*, Yunbin Han[1,2], Hao Liu[1], Haifeng Chen[1], Fuqiang Ma[1,3], Stephen G. Withers[4], Yan

[1]State Key Laboratory of Microbial Metabolism, Joint International Research Laboratory of Metabolic & Developmental Sciences, School of Life Sciences and Biotechnology, Shanghai Jiao Tong University, Shanghai 200240, China. [2]State Key Laboratory Cultivation Base for TCM Quality and Efficacy, College of Pharmacy, Nanjing University of Chinese Medicine, Nanjing 210023, China. [3]CAS Key Laboratory of Biomedical Diagnostics, Suzhou Institute of Biomedical Engineering and Technology, Chinese Academy of Sciences, China. [4]Department of Chemistry, University of British Columbia, 2036 Main Mall, Vancouver, British Columbia V6T 1Z1, Canada.
*These authors contributed equally to this work.
†Corresponding author. Email: yanggy@sjtu.edu.cn

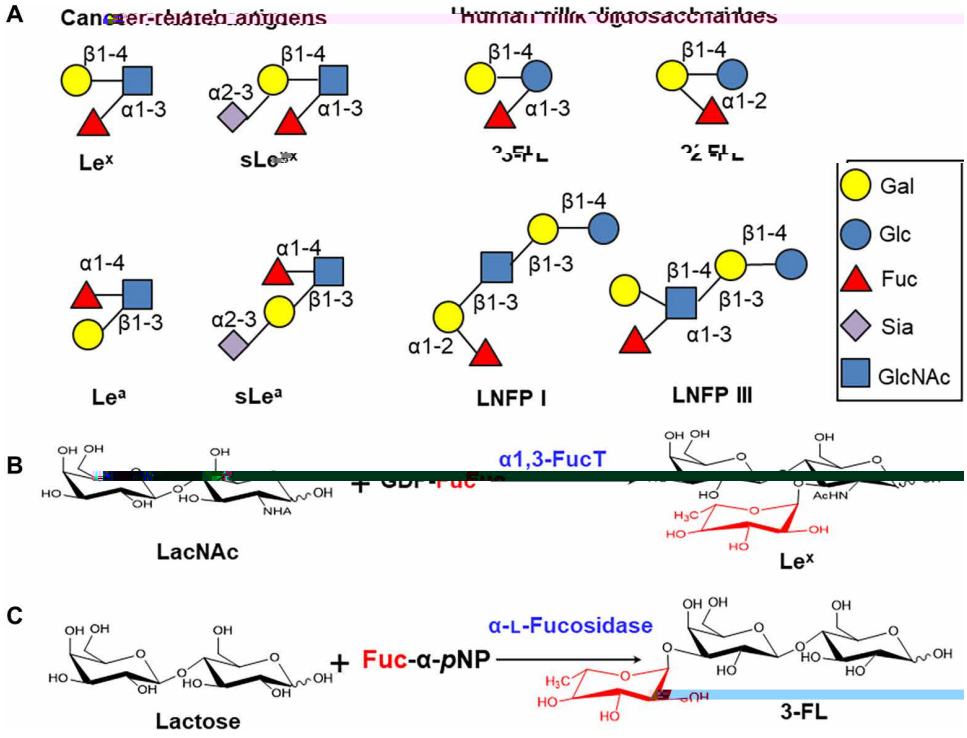

Fig. 1. Fucosylation reactions catalyzed by fucosylation enzymes. (**A**) Structures of various disease-associated and human milk oligosaccharides. (**B**) Schematic depiction of fucosylation reactions catalyzed by FucTs and fucosidases. Typically, an FutA catalyzes the L-fucose transfer from a GDP-Fuc donor substrate to a LacNAc acceptor substrate via an α1,3-linkage, forming the Le^x. α-L-Fucosidases can also transfer a fucose moiety from the para-nitrophenyl α-L-fucopyranoside (Fuc-α- NP) to lactose, forming a 3-fucosyllactose.

RESULTS

LacY substrate specificity for various fucosylated products

Helicobacter pylori 1163 (81031.1) (*15*) . 1 2 (.2). - *E. coli* 107*, ( ) ( ) (*12*) - - -1- . , *E. coli* (*23*), . ., , (*20*, *21*), (.2). , - 18 1 2. - ( ) , ( ) (.2). , ( ) ( ) (.2). - *H. pylori* (*19*) *Anaerolinea thermophila* (*22*), (. 1) . (. 1,). , , , , , (*24*).

Fig. 2. Scheme for the product entrapment strategy and the established cell-based fucosylation assay for FACS screening. (**A**) Two kinds of fluorescently labeled LacNAc derivatives (1 and 2) were designed and synthesized for cell entrapment analysis. (**B**) Fluorescently labeled acceptor substrates are transported into the cell via LacY; fucose enters into the cell via a fucosyl transporter (FucP) and was converted into GDP-fucose donor substrate by GDP-fucose synthase (FKP). After incubation and washing, *E.* cells expressing fucosylation enzymes accumulate fluorescent trisaccharide enzyme products, as the LacY transport rate for such products is significantly reduced compared to their disaccharide substrate form. Thus, the fluorescence intensity accumulation inside cells carries information about the catalytic activity of the fucosylation enzymes being assayed/screened. These cells with FutA activity can be further isolated using FACS. (**C**) Visualization of fluorescence entrapment within FutA$^{(+)}$ and FutA$^{(-)}$ cells under an ultraviolet light. (**D**) Flow cytometry profiles of FutA$^{(+)}$ and FutA$^{(-)}$ cell fluorescence after 30-min incubation with 1.5 mM fucose, 0.5 mM bodipy-LacNAc, and coumarin-LacNAc, followed by a washing step. Green and blue signals represent cells retaining bodipy and coumarin fluorescently labeled oligosaccharides, respectively.

, *E. coli*

( ),

37 30 ,

15, 8.6, 20.3%,

(. 2).

(. 2).

1

(. 3).

18

(. 3).

1

1.5 .

0.5 (. 3). ,

1.5

0.5 (. 3).

Evaluation of the FACS-based fucosylation activity screening system

.

(+)

( )

.

1 10, 1 100, 1 1000,

1 10,000 (+)/ ( ) .

,

0.5%

.

,

.

100% (+) ,

1 10,000 (1).

40 330
(*25 27*), ≳ 10,000-
.
(+)
,
( )
, *E. coli*
(+)
(.3).
( )
. , 13 ( ) 18
-
, (+)_ .
- ( )
(+)_
(+) (+)
.
((( ), / -

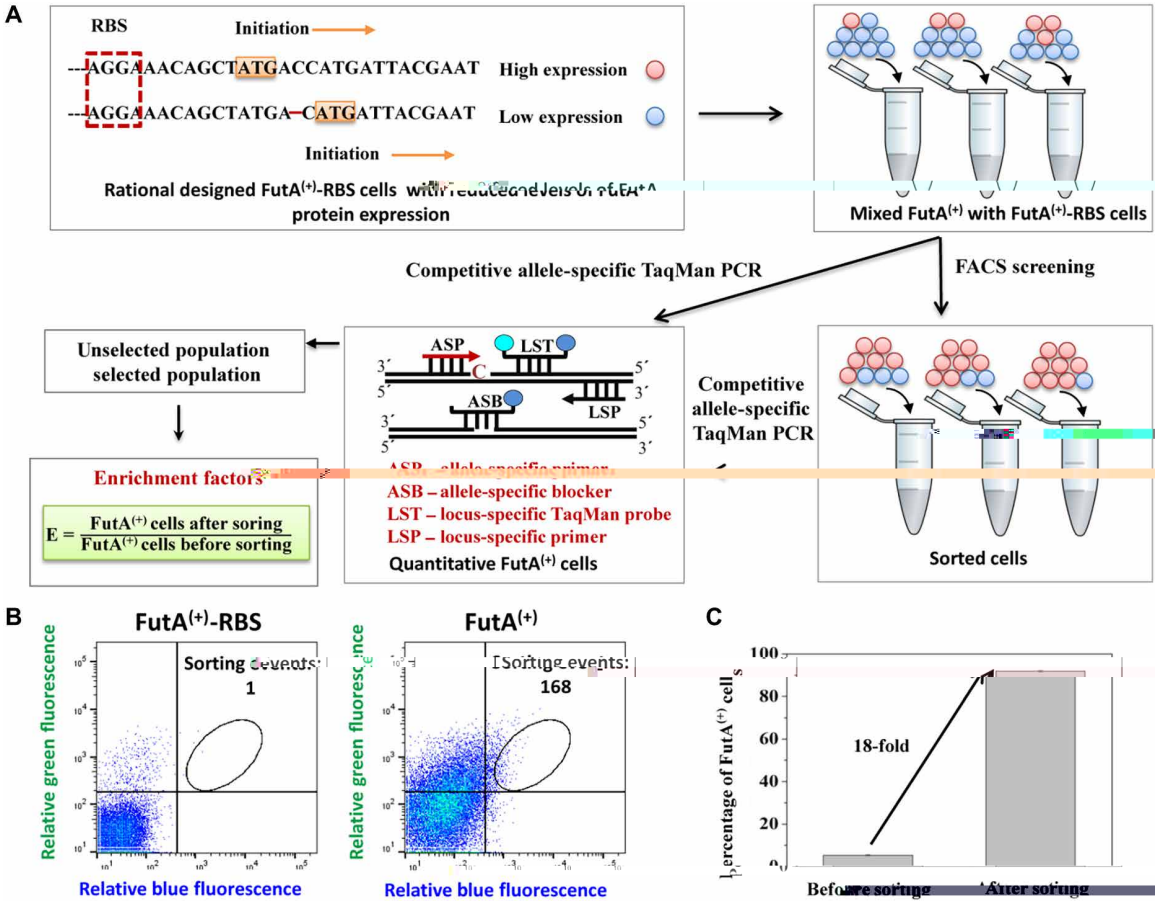

Fig. 3. Analysis of FACS-based screening efficiency by competitive allele-specific TaqMan PCR. (**A**) The RBS-ATG spacing technique was used to create two populations of cells: (i) normal FutA$^{(+)}$ cells and (ii) FutA$^{(+)}$ cells with a weakened FutA activity resulting from reduced FutA expression [FutA$^{(+)}$-RBS cells]. Cell mixtures of FutA$^{(+)}$ and FutA$^{(+)}$-RBS were prepared and applied to one round of FACS sorting. The unsorted and sorted variant pools were quantified using competitive allele-specific TaqMan PCR, and then, enrichment factors were calculated according to FutA$^{(+)}$ cell ratios before and after sorting. (**B**) Flow cytometric screening of FutA$^{(+)}$ and FutA$^{(+)}$-RBS cells. (**C**) Percentage of FutA$^{(+)}$ cells increased after sorting.

Structural analysis of the best mutant M32

, - 522.1 / - 3.6 , . 32, - 3.12 32 (. 6), 32 - . (5) - . - 115 (*31*). 32 , - , 0.82 - , 26 351 (. 8). - , 32 . , - ( ) , 20 150 . 4.1- k_{cat}/K_m 160 320 , 26 k_{cat} , (. 8). 32 , K_m . (127 / 128 / 131) (45 , 127 , 128 , , k_{cat}/K_m 131) (α2 α5) 32 (.4). 8 . k_{cat}/K_m 32 . , 1 10.8- K_m - , , 340 . k_{cat} - 6.2- K_m (1). 32 .

Table 1. Kinetic parameters for wild-type FutA and selected beneficial mutants. The kinetic assays were performed in three independent replicates, and the fitting curves for the kinetic parameters are presented in fig. S7.

	LacNAc*			GDP-Fuc†			Lactose*			GDP-Fuc†		
Enzyme	***k*cat (s^{-1})**	**K_M (mM)**	***k*cat/K_M (s^{-1} mM^{-1})**	***k*cat (s^{-1})**	**K_M (mM)**	***k*cat/K_M (s^{-1} mM^{-1})**	***k*cat (s^{-1})**	**K_M (mM)**	***k*cat/K_M (s^{-1} mM^{-1})**	***k*cat (s^{-1})**	**K_M (mM)**	***k*cat/K_M (s^{-1} mM^{-1})**
Wild type	7.91 ± 0.18	0.52 ± 0.05	15.28 ± 1.13	16.28 ± 0.62	0.09 ± 0.01	180.89 ± 13.40	1.24 ± 0.05	99.60 ± 0.08	0.01 ± 0.005	0.05 ± 0.01	0.02 ± 0.01	2.53 ± 0.28
M26	30.60 ± 0.04	0.49 ± 0.02	62.45 ± 1.74	25.97 ± 0.57	0.08 ± 0.01	324.63 ± 17.34	1.27 ± 0.02	24.30 ± 1.00	0.05 ± 0.001	0.22 ± 0.01	0.03 ± 0.01	7.35 ± 0.39
M32	34.27 ± 0.70	0.37 ± 0.04	92.62 ± 8.23	30.03 ± 0.04	0.08 ± 0.01	375.38 ± 13.81	1.26 ± 0.03	9.20 ± 1.00	0.14 ± 0.01	0.31 ± 0.01	0.02 ± 0.01	15.59 ± 1.31

*Kinetic measurements at a non-limiting concentration of the fucosyl donor substrate GDP-Fuc (0.4 mM) but variable concentrations of the acceptors LacNAc (0.02 to 8 mM) or lactose (4 to 20 mM). †Kinetic measurements at non-limiting concentrations of the acceptors LacNAc or lactose (both 0.4 mM) but a variable concentration of the fucosyl donor substrate GDP-Fuc (0.02 to 8 mM).

33 34 . 45 α2 32 - 33 34 (.4).

, *K* 32 - . - (10), - .M , α5 127 / 128 / 131 - (.4 . 8). 127 / 128 / 131 - α5 (.4). 32 , *k* . - 32- 100- ( ) - (. 8). . 20,000 5- α5 2.6 (. 8). (132 168) α5 2 (.4), α5. 32 α5 . , 1 - (-) (.4), . ,

32 , - . 340 368 , .

DISCUSSION

(*32*, *33*), . *et al.* (*31*) 1,3- 6- . - , . - - . , α2,3- (*12*) β1,3- (*14*). , . . *E. coli* (*20*, *34*), (*21*, *35*). (*35*) - — , *E. coli* (*20*). . , , . , 2- 3- .M , - (.4), .

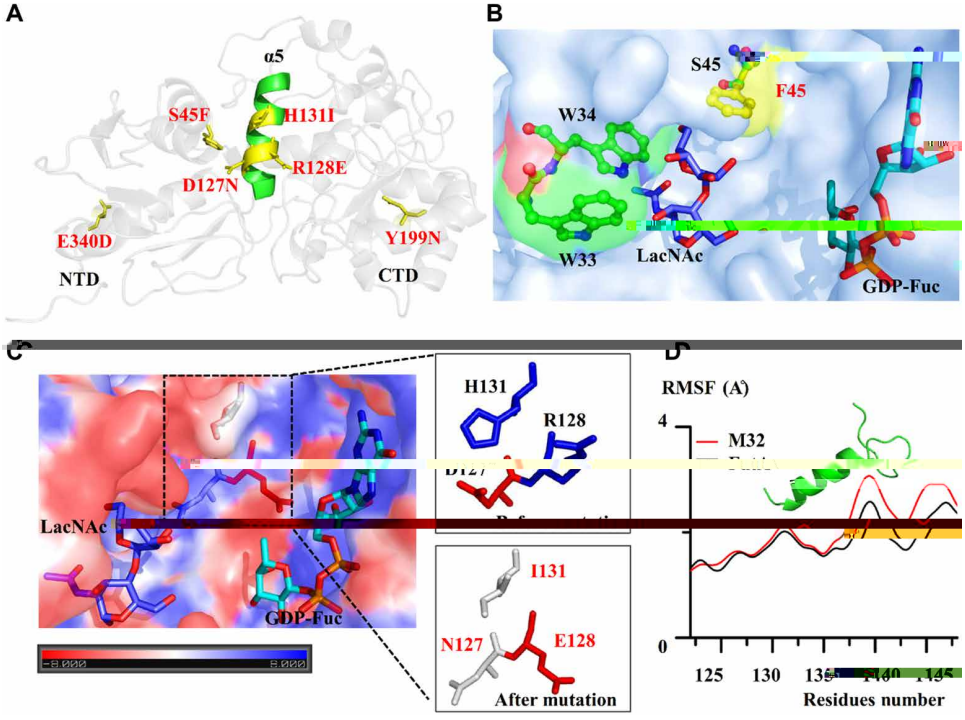

Fig. 4. Structural insight into the improved catalytic activity of the best M32 mutant. (**A**) Backbone diagram of the M32 mutant (PDB code 5ZOI) with mutations accumulations during directed evolution. Mutated residues are depicted in yellow sticks. Helix α5 having the triple mutations D127N/R128E/H131I located between the NTD and CTD is colored in green. (**B**) Enhanced interaction toward the LacNAc acceptor in the M32 mutant. The S45F mutation of M32 resulted in a new clamp-like structure with W33 and W34 at the bottom of the substrate-binding pocket. Key aromatic residues and S45 are shown in green sticks, and substituted residue F45 was represented in yellow stick. (**C**) Local electrostatic surface of M32 active pocket (red, electronegative; blue, electropositive; contoured from −8 to 8 kT/e). These D127N/R128E/H131I mutations showed a changed local electrostatic potential environment on the surface of hinge helix α5. (**D**) Root mean square fluctuation (RMSF) of wild-type FutA and M32 mutant residues from 122 to 148 region backbones in 100 ns constrained MD simulation. The segment of 122 to 148 residues are shown in cartoon.

(*32*, *33*). (*36*). 3- (*37*). 6- 14- 3- 32 45 , 127 , 128 , 131) 10 45 , 33 34,

46
H. pylori 266 5 (*31*).
, - ,
(2 7 4) (*38*) (2 7 70) (*39*),
( ) -
(*40*), -
. , 127 , 128 ,
131 ,
- . ,
- ,
(. 8). -
, -
- . ,
, -
, ,
. *E. coli* ,
. , ,
, ’ -
. , -
. ,
, ,
(. .,)
.

MATERIALS AND METHODS

Generation of random mutagenesis library

1 421
- 0 0.3 $^{2+}$
0.03 18- .
4.
18
Hind *EcoR* ,
E. coli 10 (,)
’ .
37
(100 /), . ~2, ~4, ~6, ~7
0, 0.1, 0.2, 0.3 $^{2+}$,
. .
1 1 1 1 *E. coli* 107*
.

Generation of ORM

, -
. 4. -
- 26 .
Dpn
( ) -
1% . -
E. coli 107* .

Docking simulation of LacNAc

(2 5)
.
3.5.
- .
2 ^{5}. 50
,
E/d 0. 7 /( ) .

Generation of the combinatorial active-site saturation test libraries

(4). ( ),
, , , . -
- -
5 3 , 30 5 15 ,
55 15 , 72 5 , 72 10 .
Dpn (,
). *E. coli* 107* .

Screening via flow cytometry

-
(*15*, *17*),
. , *E. coli* 107
(*12*, *14*) 18-
- 107*.
(18-) 107* (100 /)
37 . 1 50
37 -
. $_{600}$ (600) 0.5 0.7,
-β-D- ( ) 1 , 20
. (2)
50 µ 1.5 (,
), 0.5

. 30 ,
, (7.4).
6000/ ( )
.
6000 / , 85-µ , (508)
405- , 515-
( ) - 450- (1) .
- ( ) ≥ 10,000 -
( ) ≥ 10,000. 1.5-
14,000*g* 30 .
- - (4) -
( ). 50 µ
11 µ , 25 µ (2), 1 µ 10
( ), 10 µ , 20 µ
(1 µ), 1 µ -
5
3 40 5 15 , 55 15 , 72 0 , 72
10 . 18
Hind *EcoR* ,
E. coli 10 ( )
, . -
E. coli 107*
. 10 ( ).

Plus/minus reference model screening

E. coli (+) ( )
18 1 10, 1 100,
1 1000, 1 10,000.
37 30 ,
(7.4). ,
E. coli 0.5%
1.5- 0.5
( ) . -
, -
13 (47)/ 13 (48).
.

Competitive allele-specific TaqMan PCR to examine FACS-based screening efficiency

(+)- 0.03 18-
. 4. *E. coli*
107*
(+)- 1 10, 1 100, 1 1000.
1 2 37 30 .
, *E. coli*
0.5% 1.5-
. - .
, -
- ,
( ), -
, - (.3 4).

E. coli 107*
(0.1, 0.5, 1, 2.5, 5, 10, 25, 100%)
, .
50 µ 25 µ
(2), 0.6 µ 10 , 0.4 µ 10 , 0.6 µ
10 , 2.4 µ 30 , 6 µ
. 5
10 2 15 58 1 ,
40 2 15 60
1 . .
(N_0) N_0.

Protein expression and purification

futA 21
( ) *E. coli* 21 (3) .
(100 /) 37 .
37
$_{600}$ 0.8 1.0, 0.5 20 .
25 - (7.5),
100 , 20 -
. -
($^{2+}$-) (- , ,
) 200 , 500 ,
100 - (8.5), 10 2- . -
-75
( ) 25 -
(8.0), 100 , 1 . ,
30- -20
( ) ~10 / .

Enzymatic activity and kinetic analysis

, / .
( ) (*26*) ,
340 , 460 .
37 5
0.1 100 - (7.5), 1 $_2$, 1
, 50 µ , 13.5 , 30
, 4 , 400 µ -
(. ., ,), .
, .
460 .
- -
, (*29*).
5.0 (.).

Crystallization

48-
- 2 3 ,
1.0 µ .
( )/
( ). -
(*41*), .

21 1 μ 16 /
25 - (7.5) 100
0.1 (6.0), 0.05 $_2$, 45% -
200. 3 2 1,
a 121.4 , *b* 121.4 , *c* 32.4 , β 0 .
- .
- 2
2 4
.

Data collection and structure determination

- ,
, , -
30% (/) - .
- 17
1 . -
, , -2000.
. - 32 -
- .
5 4 .
32- - 32
. -
, . .
, ,
5 4 .
(*42*). -
5. (.
.) .

MD simulation

14
12 .
10 ,
. 8
- .
-
- -
(*43*).
2 . 500
3500
2 8 (,
) . 10-
, (-
, ,) 2 8 .

SUPPLEMENTARY MATERIALS

Supplementary material for this article is available at http://advances.sciencemag.org/cgi/content/full/5/10/eaaw8451/DC1

Fig. S1. Scheme for the fluorescent product entrapment strategy and the cell-based FutC and FucD fucosylation assays using FACS.
Fig. S2. Analysis of fluorescence retention in various cells.
Fig. S3. Optimization of the FACS-based system.
Fig. S4. Site-directed mutagenesis and ordered recombination of the mutation site.
Fig. S5. Rational selection of candidates for "best hit" from C_α of catalytic key residue and clustering of α helices on substrate-binding sites for CAST and SSM.
Fig. S6. LC-MS analyses of the Le^X from LacNAc catalyzed by FutA variants.
Fig. S7. Steady-state kinetics of wild type, M26, and M32 measured using various substrates.
Fig. S8. Structural insight into the improved activity of the best M32 mutant.
Table S1. Model screening of $FutA^{(+)}$ cells.
Table S2. Specific activities of FutA and selected mutants using LacNAc and lactose as acceptors.
Table S3. Activity comparison between the best mutant in the present study and previously reported FutA enzymes.
Table S4. Primers used in this study.
Table S5. Data collection and refinement statistics.
References (*44*, *45*)
View/request a protocol for this paper from *Bio-protocol*.

REFERENCES AND NOTES

1. B. Ma, J. L. Simalagrant, D. E. Taylor, Fucosylation in prokaryotes and eukaryotes. *G* **16**, 158R–184R (2006).
2. E. Miyoshi, K. Moriwaki, T. Nakagawa, Biological function of fucosylation in cancer biology. *J. B* . **143**, 725–729 (2008).
3. M. N. Christiansen, J. Chik, L. Lee, M. Anugraham, J. L. Abrahams, N. H. Packer, Cell surface protein glycosylation in cancer. *P* **14**, 525–546 (2014).
4. E. Miyoshi, K. Moriwaki, N. Terao, C.-C. Tan, M. Terao, T. Nakagawa, H. Matsumoto, S. Shinzaki, Y. Kamada, Fucosylation is a promising target for cancer diagnosis and therapy. *B* **2**, 34–45 (2012).
5. L. Bode, Human milk oligosaccharides: Every baby needs a sugar mama. *G* **22**, 1147–1162 (2012).
6. C. Kunz, S. Rudloff, W. Baier, N. Klein, S. Strobel, Oligosaccharides in human milk: Structural, functional, and metabolic aspects. *A* . *R* . *N* . **20**, 699–722 (2000).
7. B. Ma, J. L. Simala-Grant, D. E. Taylor, Fucosylation in prokaryotes and eukaryotes. *G* **12**, 158–184 (2006).
8. J. R. Díaz, R. J. Carbajo, A. P. Lucena, V. Monedero, M. J. Yebraa, Synthesis of fucosyl-*N*-Acetylglucosamine disaccharides by transfucosylation using α-L-Fucosidases from *L* . *A* . *E* . *M* . **79**, 3847–3850 (2013).
9. F. H. Arnold, Design by directed evolution. *A* . *C* . *R* . **31**, 125–131 (1998).
10. U. T. Bornscheuer, M. Pohl, Improved biocatalysts by directed evolution and rational protein design. *C* . *O* . *C* . *B* . **5**, 137–143 (2001).
11. M. S. Packer, D. R. Liu, Methods for the directed evolution of proteins. *N* . *R* . *G* . **16**, 379–394 (2015).
12. A. Aharoni, K. Thieme, C. P. C. Chiu, S. Buchini, L. L. Lairson, H. Chen, N. C. J. Strynadka, W. W. Wakarchuk, S. G. Withers, High-throughput screening methodology for the directed evolution of glycosyltransferases. *N* . *M* **3**, 609–614 (2006).
13. G. Yang, S. G. Withers, Ultrahigh-throughput FACS-based screening for directed enzyme evolution. *C* **10**, 2704–2715 (2010).
14. G. Yang, J. R. Rich, G. Michel, W. W. Wakarchuk, Y. Feng, S. G. Withers, Fluorescence activated cell sorting as a general ultra-high-throughput screening method for directed evolution of glycosyltransferases. *J. A* . *C* . . **132**, 10570–10577 (2010).
15. Z. Ge, N. W. Chan, M. M. Palcic, D. E. Taylor, Cloning and heterologous expression of an α1,3-fucosyltransferase gene from the gastric pathogen *H* . *J. B* . *C* . **272**, 21357–21363 (1997).
16. S. L. Martin, M. R. Edbrooke, T. C. Hodgman, D. H. van den Eijnden, M. I. Bird, Lewis X biosynthesis in *H* . Molecular cloning of an α(1,3)-fucosyltransferase gene. *J. B* . *C* . **272**, 21349–21356 (1997).
17. D. A. Rasko, G. Wang, M. M. Palcic, D. E. Taylor, Cloning and Characterization of the α(1,3/4) Fucosyltransferase of *H* . *J. B* . *C* . **275**, 4988–4994 (2000).
18. L. Engels, L. Elling, WbgL: A novel bacterial α1,2-fucosyltransferase for the synthesis of 2′-fucosyllactose. *G* **24**, 170–178 (2014).
19. D. B. Stein, Y. N. Lin, C. H. Lin, Characterization of *H* α1,2-fucosyltransferase for enzymatic synthesis of tumor-associated antigens. *A* . . *C* . **350**, 2313–2321 (2010).
20. J. Abramson, I. Smirnova, V. Kasho, G. Verner, H. R. Kaback, S. Iwata, Structure and mechanism of the lactose permease of *E* . **301**, 610–615 (2003).
21. I. Smirnova, V. Kasho, X. Jiang, H. M. Chen, S. G. Withers, H. R. Kaback, Oversized galactosides as a probe for conformational dynamics in LacY. *P* . *N* . *A* . . . . *A.* **115**, 4146–4151 (2018).
22. M. Lezyk, C. Jers, L. Kjaerulff, C. H. Gotfredsen, M. D. Mikkelsen, J. D. Mikkelsen, Novel α-L-fucosidases from a soil metagenome for production of fucosylated human milk oligosaccharides. *PLO ONE* **11**, e0147438 (2016).
23. M. H. Saier Jr., Families of transmembrane sugar transport proteins. *M* . *M* . **35**, 699–710 (2010).

24. Y. Sun, C. K. Vanderpool, Regulation and function of *E* sugar efflux transporter A (SetA) during glucose-phosphate stress. *J. B* . **193**, 143–153 (2011).
25. A. Amir, A. Gil, B. Kalia, M. Shlomo, S. D. Tawfik, High-throughput screening of enzyme libraries: Thiolactonases evolved by fluorescence-activated sorting of single cells in emulsion compartments. *C* . *B* . **12**, 1281–1289 (2005).
26. E. Mastrobattista, V. Taly, E. Chanudet, P. Treacy, B. T. Kelly, A. D. Griffiths, High-throughput screening of enzyme libraries: In vitro evolution of a β-ga4485 0 BT1-n5llveres1 1 6.5 36 691.3851 Tm3.26699 -7.9925 Td( )TjEMC ET-35.6865 Td(throughpence-activated sorting of)TjE

Directed evolution of an α1,3-fucosyltransferase using a single-cell ultrahigh-throughput screening method

Yumeng Tan, Yong Zhang, Yunbin Han, Hao Liu, Haifeng Chen, Fuqiang Ma, Stephen G. Withers, Yan Feng and Guangyu Yang

Sci Adv **5** (10), eaaw8451.
DOI: 10.1126/sciadv.aaw8451